

On the Convergence of the Born Series in Optical Tomography with Diffuse Light

Vadim A. Markel[†]

Departments of Radiology and Bioengineering, University of Pennsylvania,
Philadelphia, PA 19104

John C. Schotland[‡]

Department of Bioengineering, University of Pennsylvania, Philadelphia, PA 19104

Abstract. We provide a simple sufficient condition for convergence of Born series in the forward problem of optical diffusion tomography. The condition does not depend on the shape or spatial extent of the inhomogeneity but only on its amplitude.

Submitted to: *Inverse Problems*

[†] E-mail: vmarkel@mail.med.upenn.edu

[‡] E-mail: schotland@seas.upenn.edu

1. Introduction

Many inverse scattering problems in imaging are known to be nonlinear. Physically, this is a manifestation of the fact that the probing waves do not propagate via well-defined trajectories. When such trajectories do exist, the inverse problem can usually be linearized as is the case, for example, in single-energy computed x-ray tomography. If the probing waves experience scattering and trajectories can not be defined in principle, nonlinearity of the inverse problem is practically unavoidable.

Mathematically, the nonlinearity of the inverse problem can be understood as the nonlinear dependence of the measured signal on the quantity of interest. In the case of optical tomography (OT), the measured signal is the intensity of light exiting from a highly-scattering sample and the quantities of interest are the absorption and the scattering coefficients. The nonlinear nature of the dependence of OT measurements on these coefficients is well-known [1, 2].

Practical approaches to solving nonlinear inverse problems can be divided into two broadly defined classes of iterative and analytic methods. Iterative methods, including the Newton-type [1, 3, 4] and Bayesian [5] methods, seek to optimize a certain cost function according to an iterative rule which typically requires solving the forward problem at each iteration step. The advantage of iterative methods is their generality, since they do not require knowledge of the analytical structure of the forward operator. Instead, the forward problem is solved at each iteration step numerically. Methods of the second class rely on some analytical manipulations with the forward operator. This includes various approximate linearization schemes which, generally, work only for weak inhomogeneities and methods based on functional series expansions. Thus, image reconstruction algorithms based on an inverse scattering series were proposed in geophysics (inverse scattering of seismic waves) [6, 7], in optical near-field imaging [8], and in OT [9].

While little is presently known about the convergence of the inverse series, a number of results on convergence of the forward series has been obtained. In quantum-mechanical scattering theory, Bushell has shown that the Born series converges if the potential is too shallow to support at least one bound state [10]. Colton and Kress have studied the convergence of the Born series for the scalar wave equation in an infinite space [11]. In particular, as part of the proof of Theorem 8.4 of Ref. [11], it is shown that the Born series converges if the susceptibility $\eta(\mathbf{r}) = n^2(\mathbf{r}) - 1$ [$n(\mathbf{r})$ being the refractive index] is bounded by $|\eta(\mathbf{r})| < 2/(ka)^2$, where $k = \omega/c$ is the wave number and a is the radius of the smallest sphere that contains the support of $\eta(\mathbf{r})$. We note that Bushell's convergence condition is indirect and, therefore, difficult to use. The convergence condition of Colton and Kress is applicable to functions of compact support but is not useful at all in the limit $ka \rightarrow \infty$. In addition, it is only applicable to scattering by a potential in free space. In this paper, we show that, in the case of the diffusion equation used in OT, a simple condition for convergence of the Born series can be obtained independently of the medium boundaries. A remarkable property of this

condition is that it is also independent of shape or support of the inhomogeneity but only depends on its amplitude. Thus, we show that the forward series expansion for the Green's function of the diffusion equation in powers of absorptive inhomogeneity $\delta\alpha(\mathbf{r})$ (the absorption coefficient is decomposed as $\alpha(\mathbf{r}) = \alpha_0 + \delta\alpha(\mathbf{r})$ where α_0 is a constant) always converges if

$$|\delta\alpha(\mathbf{r})| \leq \alpha_0 . \quad (1)$$

A similar condition is obtained for the diffusion coefficient $D(\mathbf{r}) = D_0 + \delta D(\mathbf{r})$. We argue that the independence of this condition on the shape or spatial extent of the inhomogeneity is a consequence of the exponential decay of diffuse waves which results in weak long-range interactions. This argument will be made more precise in Section 5 below and illustrated numerically in Section 7.

The convergence condition (1) is obtained independently of restrictions on the support of the inhomogeneities or of the nature of medium boundaries. However, if the support of the inhomogeneity is contained in a finite ball of radius a and the system is embedded in an infinite homogeneous medium, we can repeat the arguments of Ref. [11] for the diffusion equation and obtain an even sharper condition on $\delta\alpha(\mathbf{r})$. Namely, we will show that, for absorbing inhomogeneities and under the conditions stated above, the Born series converges if

$$\delta\alpha(\mathbf{r}) < \frac{\alpha_0}{1 - (1 + k_d a) \exp(-k_d a)} , \quad (2)$$

where $k_d = \sqrt{\alpha_0/D_0}$ is the diffuse wave number (the analog of the wave number k of the scalar wave equation). It can be seen that in the limit $k_d a \rightarrow \infty$, we reproduce the condition $\delta\alpha < \alpha_0$, while in the limit $k_d a \rightarrow 0$, we reproduce Colton and Kress' condition $\delta\alpha < 2\alpha_0/(k_d a)^2$ (note that $\delta\alpha/\alpha_0$ is the direct analog of the susceptibility η of the scalar wave equation considered by Colton and Kress).

The paper is organized as follows. In Section 2 we define the problem of OT, review the mathematical formalism that leads to the Born series expansions and introduce the relevant notation. In Sections 3 and 4 we obtain the convergence condition of the type (1) for absorbing and scattering inhomogeneities, respectively. In Section 5 we generalize the Colton and Kress' result for the case of the diffusion equation with an absorbing inhomogeneity embedded in an infinite homogeneous medium and derive the convergence condition (2). In Section 6 we describe a discretization scheme for representation of operators by matrices which is used in numerical examples of Section 7. Here the analytical results of Section 3 are verified numerically. Finally, Section 8 contains a discussion of obtained results.

Before proceeding with the main content of this paper, we wish to clarify the following point. In the text below, we use the terms “multiple scattering of diffuse waves” and “interaction”. We are referring to multiple scattering of scalar solutions to the diffusion equation from inhomogeneities in its coefficients – not to multiple scattering of electromagnetic waves from inhomogeneities in the dielectric susceptibility. The first

effect can be viewed as macroscopic, and takes place on much larger scales than the second effect. In particular, a macroscopically homogeneous medium with constant absorption and diffusion coefficients exhibits no scattering of diffuse waves, although the very possibility to describe the electromagnetic energy density by the diffusion equation is based on the assumption of strong multiple scattering of electromagnetic waves on microscopic physical scales. Similarly, by “interaction” we mean the interaction (interference and multiple scattering) of diffuse waves scattered from macroscopic inhomogeneities.

2. Derivation of the Born Series

Propagation of light in biological tissues is commonly described by the diffusion approximation to the radiative transport equation [1,2]. In the case of continuous-wave illumination, the following steady-state diffusion equation is used:

$$[-\nabla \cdot D(\mathbf{r})\nabla + \alpha(\mathbf{r})]u(\mathbf{r}) = q(\mathbf{r}) , \quad (3)$$

where u is the energy density of the diffuse light inside the medium, q is the source function, $D = c/[3(\mu_a + \mu'_s)]$, $\alpha = c\mu_a$ and c is the average speed of light in the medium. Further, μ_a and μ'_s are the absorption and reduces scattering coefficients, respectively. Reconstruction of the functions $\mu_a(\mathbf{r})$ and $\mu'_s(\mathbf{r})$ from a set of boundary measurements is the goal of OT.

Experiments in OT are usually performed with point sources (plane-wave [12] or structured [13] illumination have also been proposed). A point source can be written as $q(\mathbf{r}) = q_0\delta(\mathbf{r} - \mathbf{r}_s)$. Here \mathbf{r}_s is the source location on the boundary of the medium. A point detector located at \mathbf{r}_d can be shown [14] to produce a measurement that is proportional to the Green's function of Eq. (3), $G(\mathbf{r}_d, \mathbf{r}_s)$, which satisfies

$$[\nabla \cdot D(\mathbf{r})\nabla - \alpha(\mathbf{r})]G(\mathbf{r}, \mathbf{r}') = -\delta(\mathbf{r} - \mathbf{r}') . \quad (4)$$

We now decompose $\alpha(\mathbf{r})$ and $D(\mathbf{r})$ as constant background values α_0 , D_0 and spatially-varying functions $\delta\alpha(\mathbf{r})$, $\delta D(\mathbf{r})$, according to $\alpha(\mathbf{r}) = \alpha_0 + \delta\alpha(\mathbf{r})$ and $D(\mathbf{r}) = D_0 + \delta D(\mathbf{r})$. The background constants are chosen to be equal to the respective values of α and D near the medium boundary where these coefficients are either directly measurable or known, i.e., by immersing the sample into a matching fluid whose optical properties are known. We then obtain the Dyson equation for the Green's function [15,16], namely

$$G(\mathbf{r}, \mathbf{r}') = G_0(\mathbf{r}, \mathbf{r}') + \int G_0(\mathbf{r}, \mathbf{r}'')V(\mathbf{r}'')G(\mathbf{r}'', \mathbf{r}')d^3r , \quad (5)$$

where the integration is over the spatial region occupied by the scattering medium, $G_0(\mathbf{r}, \mathbf{r}')$ is the Green's function for a homogeneous medium with $\alpha = \alpha_0$ and $D = D_0$, i.e., it satisfies

$$[D_0\nabla^2 - \alpha_0]G_0(\mathbf{r}, \mathbf{r}') = -\delta(\mathbf{r} - \mathbf{r}') \quad (6)$$

and appropriate boundary conditions on the scattering medium boundary, and $V(\mathbf{r})$ is given by

$$V(\mathbf{r}) = V_\alpha(\mathbf{r}) + V_D(\mathbf{r}) , \quad (7)$$

$$V_\alpha(\mathbf{r}) = -\delta\alpha(\mathbf{r}) , \quad (8)$$

$$V_D(\mathbf{r}) = -\mathbf{p} \cdot \delta D(\mathbf{r}) \mathbf{p} . \quad (9)$$

Here we have introduced the momentum operator $\mathbf{p} = -i\nabla$. Since \mathbf{p} is Hermitian (self-adjoint), so is V_D . We note that the Dyson equation (5) is valid for \mathbf{r} , \mathbf{r}' being inside the scattering medium or on its boundary. In the latter case, we can replace \mathbf{r} and \mathbf{r}' by \mathbf{r}_d and \mathbf{r}_s .

In operator notation, the Dyson equation (5) is written as

$$G = G_0 + G_0 V G , \quad (10)$$

where $V = V_\alpha + V_D$ is the interaction operator. We note that V_α is diagonal in the position representation and has the matrix elements

$$\langle \mathbf{r} | V_\alpha | \mathbf{r}' \rangle = -\delta\alpha(\mathbf{r}) \delta(\mathbf{r} - \mathbf{r}') . \quad (11)$$

However, V_D has no position representation. § Its matrix elements can be defined in the basis of plane waves (in \mathbf{k} -space). For example, in an infinite space we can take the basis functions to be $|\psi_{\mathbf{k}}\rangle$, such that $\langle \mathbf{r} | \psi_{\mathbf{k}} \rangle = (2\pi)^{-3/2} \exp(i\mathbf{k} \cdot \mathbf{r})$, Then we have the following matrix elements (of both V_α and V_D):

$$\langle \psi_{\mathbf{k}'} | V_\alpha | \psi_{\mathbf{k}} \rangle = -\delta\tilde{\alpha}(\mathbf{k} - \mathbf{k}') , \quad (12)$$

$$\langle \psi_{\mathbf{k}'} | V_D | \psi_{\mathbf{k}} \rangle = -\mathbf{k}' \cdot \mathbf{k} \delta\tilde{D}(\mathbf{k} - \mathbf{k}') , \quad (13)$$

where the tilde denotes three-dimensional Fourier transform with respect to the spatial variable \mathbf{r} . The simple mathematical structure of the above matrix elements suggests that the forward and inverse problems are more naturally formulated in \mathbf{k} -space, especially if the medium boundaries are translationally invariant [14, 17].

The Born series is obtained by iterating (10) starting with $G = G_0$ and has the form

$$G = G_0 + G_0 V G_0 + G_0 V G_0 V G_0 + \dots = G_0 \sum_{k=0}^{\infty} (V G_0)^k . \quad (14)$$

The Born series can also be viewed as the Taylor expansion of the formal solution to (10) into a power series in V ,

$$G = (I - G_0 V)^{-1} G_0 = G_0 (I - V G_0)^{-1} , \quad (15)$$

§ Of course, differential operators in Eq. (3) can be approximated by finite differences. However, all finite difference schemes are non-local (involve several spatial points) and, strictly speaking, can not be used to define a position representation of V_D .

I being the identity operator.

The derivation of the convergence condition can be obtained directly starting from Eq. (15). However, a more mathematically elegant approach can be based on an analogous formula for the T-matrix. In the T-matrix formalism, one writes the Dyson equation (10) as

$$G = G_0 + G_0 T G_0 . \quad (16)$$

From the identity $T G_0 = V G$, we obtain $T = V G G_0^{-1}$ or, substituting this into (15),

$$T = V(I - G_0 V)^{-1} = (I - V G_0)^{-1} V . \quad (17)$$

The Born series for the T-matrix is

$$T = V + V G_0 V + V G_0 V G_0 V + \dots = \left[\sum_{k=0}^{\infty} (V G_0)^k \right] V . \quad (18)$$

Note that the series in (14) and (18) are identical and, therefore, the convergence conditions for the series expansions of G and T are also identical.

3. The Convergence Condition for Absorbing Inhomogeneities

The diffusion approximation is valid when $\mu'_s \gg \mu_a$. If, in addition, μ'_s is constant inside the sample, then $D(\mathbf{r})$ is also, approximately, constant. This case is practically important when the contrast mechanism is directly related to absorption, but not to scattering, for instance, in imaging of blood oxygenation levels [18].

In this Section, we specialize to the case $\delta D = 0$, $\delta\alpha \neq 0$, so that $V = V_\alpha$. We say that the function $\delta\alpha(\mathbf{r})$ is *physically allowable* if $\delta\alpha(\mathbf{r}) \geq -\alpha_0$. In the opposite case, the total absorption coefficient $\alpha(\mathbf{r}) = \alpha_0 + \delta\alpha(\mathbf{r})$ can become negative, which physically corresponds to an amplifying medium.

The derivations presented below are based on the assumption that for any physically allowable $\delta\alpha$, the diffusion equation (3) has a solution. We also use the fact that if $\delta\alpha$ is physically allowable and satisfies $\delta\alpha \leq \alpha_0$, then $-\delta\alpha$ is also physically allowable. While we assume on physical grounds that Eq. (3) has a solution for every physically allowable $\delta\alpha$, it can not be stated that if $\delta\alpha$ is *not physically allowable*, then (3) *has no solutions*. In fact, (3) can have a steady-state solution even if the medium is amplifying in some finite spatial region, as long as there also exists a sufficiently strong energy sink ¶. For this reason, the convergence conditions derived in Sections 3,4 are sufficient but not necessary.

¶ If $D = D_0 = \text{const}$, the diffusion equation (3) is mathematically equivalent to the Schroedinger equation for a single particle of mass m in the potential $U(\mathbf{r}) = (\hbar^2/2m)\alpha(\mathbf{r})/D_0$. From the analysis presented below, it will be clear that the solution to (3) ceases to exist if the potential $U(\mathbf{r})$ is deep enough to support at least one bound state. See Ref. [10] for a similar argument.

3.1. Sign-Definite $\delta\alpha$.

We start with the simple case of a sign-definite function $\delta\alpha(\mathbf{r})$. Namely, we assume that $\delta\alpha(\mathbf{r})$ does not change sign within its domain (but can be zero). We also assume that $\delta\alpha(\mathbf{r})$ has no singularities. Then we can write

$$V = -\sigma SS, \quad (19)$$

where $\sigma = \pm 1$ and S is a non-negative definite operator, diagonal in the position representation. The values of σ are $\sigma = +1$ if $\delta\alpha \geq 0$ and $\sigma = -1$ if $\delta\alpha \leq 0$. Then, with little algebraic manipulation, we obtain

$$T = -\sigma S(I + \sigma SG_0 S)^{-1} S = -\sigma S(I + \sigma W)^{-1} S. \quad (20)$$

In the above formula, $W = SG_0 S$. The matrix elements of W are given by

$$\langle \mathbf{r} | W | \mathbf{r}' \rangle = \sqrt{|\delta\alpha(\mathbf{r})|} G_0(\mathbf{r}, \mathbf{r}') \sqrt{|\delta\alpha(\mathbf{r}')|}. \quad (21)$$

The operator W can be viewed as a functional of $\delta\alpha$. We note the following obvious property: $W[\gamma\delta\alpha] = |\gamma|W[|\delta\alpha|]$, where γ is a constant.

W is real and symmetric so that all of its eigenvalues w_μ are real. The Born series (18) converges if all eigenvalues satisfy $|w_\mu| < 1$ and diverges otherwise. We note that the index μ that labels the eigenvalues may not be countable, i.e., if the spectrum of W is continuous. Of course, the eigenvalues w_μ are not computable analytically in general and the above condition is of little practical use. However, we will employ the following lemma to obtain conditions on $\delta\alpha$ itself:

Lemma 1 For any physically allowable $\delta\alpha$ that does not change sign, $\sigma w_\mu[\delta\alpha] \neq -1$ for all indices μ .

Proof For any physically allowable $\delta\alpha$, there is a solution to the diffusion equation (3) and, correspondingly, a T-matrix. For the T-matrix to exist, the operator $I + \sigma W$ in (21) must be invertible. But if $\sigma w_\mu = -1$ for at least one eigenvalue, the above operator is not invertible.

In particular, for non-negative functions $\delta\alpha$ ($\sigma = +1$), $w_\mu[\delta\alpha] \neq -1$ and for non-positive and *physically allowable* functions $\delta\alpha$ ($\sigma = -1$), $w_\mu[\delta\alpha] \neq +1$. If the sign of a physically allowable $\delta\alpha$ is reversed and $-\delta\alpha$ is still physically allowable, then $w_\mu[\delta\alpha] \neq \pm 1$. This property holds for all physically allowable functions $\delta\alpha$ such that $\delta\alpha \leq \alpha_0$.

We can now state two simple results that set bounds on the spectrum of W .

Proposition 1 For any physically allowable $\delta\alpha$ that does not change sign, $W[\delta\alpha]$ has no negative eigenvalues.

Proof Let $W[\delta\alpha]$ have an eigenvalue $w < 0$. Choose $\gamma = 1/|w|$. Then $W[\gamma|\delta\alpha|]$ has an eigenvalue -1 . Since $\gamma|\delta\alpha|$ is non-negative, this is not possible by Lemma 1.

Proposition 2 If, in addition to the conditions of Proposition 1, $\delta\alpha \leq \alpha_0$, then all eigenvalues of $W[\delta\alpha]$ are less than unity.

Proof Let $W[\delta\alpha]$ have an eigenvalue $w > 1$. Choose $\gamma = -1/w$. Then $W[\gamma|\delta\alpha|]$ has an eigenvalue $+1$. Since $\gamma|\delta\alpha|$ is physically allowable and non-positive, this is not possible by Lemma 1.

To summarize, we have found that all eigenvalues of the matrix $W = SG_0S$ lie in the open interval $[0, 1)$ for all physically allowable functions $\delta\alpha$ that satisfy the conditions of Proposition 2. Since $\sigma = \pm 1$, we immediately conclude that, under the same conditions, the expansion of (20) into a power series in W converges. It is further straightforward to see that this expansion is identical to (18) or (14). Therefore, we have established the following condition for convergence of the Born series:

Theorem The Born series for the T-matrix or the Green's function converges if (i) $\delta\alpha$ is physically allowable, (ii) does not change sign inside its domain, and (iii) satisfies $\delta\alpha(\mathbf{r}) \leq \alpha_0$.

A remarkable feature of the above condition is that it depends only on the upper bound for $\delta\alpha$, but not on its shape or spatial extent. Thus, for example, let $\delta\alpha(\mathbf{r}) = A \leq \alpha_0$ inside some region Ω . The Born series will converge independently of the shape or linear dimensions of this region. Physically, this can be understood by considering the fact that $G_0(\mathbf{r}, \mathbf{r}')$ decays exponentially with the distance between \mathbf{r} and \mathbf{r}' . Therefore, multiple scattering of diffuse waves on large scales is exponentially suppressed. Instead, scattering is strong at small scales, when $G_0(\mathbf{r}, \mathbf{r}') \propto 1/|\mathbf{r} - \mathbf{r}'|$. It is this short-range interaction that may result in a substantially nonlinear dependence of $G(V)$ or $T(V)$ on V . If $\delta\alpha/\alpha_0$ is sufficiently large, even locally, the nonlinearity may become so strong that the power series expansion of $T(V)$ does not converge. However, we have established that this expansion always converges if $\delta\alpha \leq \alpha_0$.

We conclude this subsection with the following remark. Proposition 1 is stronger than is needed for the derivation of the above convergence condition. The inequality $w_\mu > -1$ would be sufficient. In fact, we will see below that Proposition 1 holds only for operators W whose trace is infinite. If we perform a discretization as is explained in Section 6, W becomes a finite-size matrix of zero trace. The scaling property $W[\gamma\delta\alpha] = |\gamma|W[|\delta\alpha|]$ does not hold for such matrices. Consequently, some of their eigenvalues are negative. However, they are all greater than -1 . The proof of this statement is very similar to the proof of Proposition 2 and is omitted; instead, we will illustrate this fact with numerical examples.

3.2. Sign-Indefinite $\delta\alpha$.

We will now show that the convergence condition formulated in the previous subsection holds even if $\delta\alpha(\mathbf{r})$ can change sign.

Before proceeding with the proof, we set the stage for the numerical verification of this statement in Section 7 below. Since $\delta\alpha$ is now allowed to change sign, we can no longer write $V = -\sigma SS$ where $\sigma = \pm 1$ and S is real and non-negative definite. Instead, we can write, for example, $V = -S_c S_c$, where S_c is complex. Analogously to (20), we have

$$T = -S_c(I + S_c G_0 S_c)^{-1} S_c = -S_c(I + W_c)^{-1} S_c, \quad (22)$$

where $W_c = S_c G_0 S_c$. The matrix elements of W_c are

$$\langle \mathbf{r} | W_c | \mathbf{r}' \rangle = \sqrt{\delta\alpha(\mathbf{r})} G_0(\mathbf{r}, \mathbf{r}') \sqrt{\delta\alpha(\mathbf{r}')}. \quad (23)$$

Note that W_c does not depend on the choice of the square root branch in the above formula, as long as the same branch is chosen in both square roots.

Since W_c is complex symmetric and hence non-Hermitian, its eigenvalues are in general complex. Therefore, placing bounds on the eigenvalues of W_c is problematic. Indeed, the analog of Lemma 1 for Eq. (22) is $w_\mu \neq -1$. But this inequality can be satisfied trivially if w_μ has an imaginary part. Therefore, Eq. (22) is not useful for the derivation of a convergence condition. Instead, we will study eigenvalues of W_c numerically in Section 7. Here we will use a different representation for the T-matrix. Namely, we can write $V = -S\Sigma S$ where S is still real and non-negative definite but Σ is now an operator rather than a number:

$$\langle \mathbf{r} | \Sigma | \mathbf{r}' \rangle = \delta(\mathbf{r} - \mathbf{r}') \begin{cases} +1, & \text{if } \delta\alpha(\mathbf{r}) \geq 0, \\ -1, & \text{if } \delta\alpha(\mathbf{r}) < 0. \end{cases} \quad (24)$$

Thus, we can refer to Σ as the sign operator. Note that Σ and S commute. After straightforward algebraic manipulation, we obtain

$$T = -S(\Sigma + S G_0 S)^{-1} S = -S(\Sigma + W)^{-1} S. \quad (25)$$

In the above equation, $W[\delta\alpha]$ is defined by (21) of Section 3.1, but its domain has been generalized to include functions $\delta\alpha$ that can change sign. Still, since $W[\delta\alpha] = W[|\delta\alpha|]$, and from the results of previous subsection, we know that the eigenvalues w_μ of W lie in the interval $[0, 1)$, as long as $|\delta\alpha| \leq \alpha_0$. Therefore, $\|W\| < 1$, where $\|\cdot\|$ is the operator norm defined here as $\|W\| = \sup[\langle \psi | W | \psi \rangle / \langle \psi | \psi \rangle]$. On the other hand, from the obvious relation $\Sigma^2 = I$, we find that $\|\Sigma\| = 1$. We then write

$$(\Sigma + W)^{-1} = [\Sigma(I + \Sigma W)]^{-1} = (I + \Sigma W)^{-1} \Sigma. \quad (26)$$

The Born series is obtained by expanding

$$(I + \Sigma W)^{-1} = \sum_{k=0}^{\infty} (-\Sigma W)^k. \quad (27)$$

From the operator norm inequality $\|AB\|_p \leq \|A\|_p \cdot \|B\|_p$, we immediately obtain $\|\Sigma W\| < 1$, which is a sufficient condition for convergence of the series (27). This completes the proof that the convergence condition of the previous subsection applies to functions $\delta\alpha(\mathbf{r})$ that can change sign.

4. The Convergence Condition for Scattering Inhomogeneities

If $\mu_a = \text{const}$ while μ'_s varies, the system is characterized by a scattering inhomogeneity. We then have $\delta\alpha = 0$, $\delta D \neq 0$. Obviously, the physically allowable values of δD satisfy $\delta D \geq -D_0$. However, the physical interpretation of what happens if we do allow $D(\mathbf{r})$ to become negative is somewhat different. If the source function of Eq. (3) is zero in the spatial region where D is negative, then the interpretation is that the medium in that region is amplifying, similar to the case of absorbing inhomogeneities. But if D is negative in a region where the source is nonzero, then, in addition to having amplifying medium, the source of energy is turned into a sink.

We now restrict consideration to a physically allowable δD and state that the convergence condition of Section 3 applies to scattering inhomogeneities with the substitution $\alpha_0 \rightarrow D_0$ and $\delta\alpha \rightarrow \delta D$. The proof of this statement is analogous to the proof given in Section 3 and will be only briefly sketched.

For a general physically allowable δD , the interaction operator can be written as $V = V_D = -\mathbf{p} \cdot S \Sigma S \mathbf{p}$ and the symmetric expression for the T-matrix, analogous to (25), is

$$T = -\mathbf{p} \cdot S [\Sigma + S \mathbf{p} G_0 \mathbf{p} \cdot S]^{-1} S \mathbf{p} . \quad (28)$$

The operator $W = S \mathbf{p} G_0 \mathbf{p} \cdot S$ is complex but Hermitian, so that all of its eigenvalues are strictly real. By considering the special cases of sign-definite δD when $\Sigma = \pm I$, we obtain bounds on the eigenvalues of W in complete analogy with Section 3.1. More specifically, the eigenvalues of W all lie in the open interval $[0, 1)$, as long as $\delta D \leq D_0$. We then find that the operator norm of W is less than unity while it is exactly unity for Σ , and, consequently, expansion of (28) into a power series converges.

5. Generalization of Colton and Kress' Result

Further insight into the convergence properties of the Born series and the strength of nonlinearity can be gained by considering the argument similar to the one used by Colton and Kress in the proof of Theorem 8.4 of Ref. [11]. The argument is based on a direct estimation of the norm $\|VG_0\|_\infty$ of the operator VG_0 that appears in the series (14) or (18). The (necessary and sufficient) convergence condition for the Born series is $\|VG_0\|_\infty < 1$. Of course, estimation of this norm is possible only if G_0 is known analytically. For a medium with boundaries, G_0 can only be computed numerically. Therefore, we will consider below the simple case of free space, so that

$$G_0(\mathbf{r}, \mathbf{r}') = G_F(\mathbf{r}, \mathbf{r}') = \frac{\exp(-k_d |\mathbf{r} - \mathbf{r}'|)}{4\pi D_0 |\mathbf{r} - \mathbf{r}'|} , \quad (29)$$

where $k_d = \sqrt{\alpha_0/D_0}$ is the diffuse wave number. However, note that the influence of boundaries can be exponentially small, as is discussed in Section 6 below.

Next, we specialize to the case of absorbing inhomogeneities, $V = V_\alpha$, where V_α is defined by (8). Assuming that $\delta\alpha(\mathbf{r}) = 0$ if \mathbf{r} is outside of a sphere of radius a , we have

$$\|VG_0\|_\infty \leq \sup_{|\mathbf{r}| \leq a} (|\delta\alpha(\mathbf{r})|) \sup_{|\mathbf{r}| \leq a} (|I(\mathbf{r})|) , \quad (30)$$

where

$$I(\mathbf{r}) = \int_{r' < a} G_F(\mathbf{r}, \mathbf{r}') d^3r' . \quad (31)$$

The above integral can be easily evaluated to yield

$$I(\mathbf{r}) = \frac{1}{D_0 k_d^2} \left[1 - (1 + k_d a) \exp(-k_d a) \frac{\exp(k_d r) - \exp(-k_d r)}{2k_d r} \right] . \quad (32)$$

Obviously, the maximum of the above function is at the center of the ball, so that

$$\sup_{|\mathbf{r}| \leq a} (|I(\mathbf{r})|) = \frac{1}{D_0 k_d^2} f(k_d a) , \quad f(x) = 1 - (1 + x) \exp(-x) . \quad (33)$$

We then immediately arrive at the (sufficient) convergence condition (2) for $\delta\alpha$.

We now examine the two limiting cases $k_d a \rightarrow 0$ and $k_d a \rightarrow \infty$. In the first case, we use $f(x) \approx x^2/2$ for small x and recover Colton and Kress' convergence condition $\delta\alpha < 2\alpha_0/(k_d a)^2$. In the second case, the domain of $\delta\alpha$ is not restricted and we recover the result of Section 3, namely, $\delta\alpha < \alpha_0$ with the only difference that we now have a strict inequality. The independence of the latter result on $k_d a$ is specific to the diffusion equation and results from the exponential decay of diffuse waves. Indeed, we have $\lim_{k_d a \rightarrow \infty} f(k_d a) = 1$. However, if we perform the analytic continuation $k_d \rightarrow ik$, the corresponding limit is $\lim_{ka \rightarrow \infty} |f(ika)| = ka$ and the convergence condition becomes $\eta < 1/ka$ (we have replaced here $\delta\alpha/\alpha_0$ by its counterpart η). This fact illustrates the crucial difference in convergence properties of the Born series for propagating and diffuse waves.

6. Discretization

In any numerical simulations, the operators G_0 , V must be discretized and truncated using some appropriate basis. Here we restrict our attention to absorptive inhomogeneities so that $V = V_\alpha$ and use the basis of cubic voxels. We note that the same discretization method can not be applied to V_D because, as was mentioned in Section 2, V_D has no position representation.

The discretization method described below is analogous to the so-called discrete-dipole approximation [19] that has been widely used in electromagnetic scattering by nonspherical particles [20, 21]. We seek to discretize the integral equation (5) in a basis of cubic voxels. Instead of working directly with (5), it is more convenient to first write the Lippmann-Schwinger integral equation for the field u itself. Let

$u(\mathbf{r}) = \int G(\mathbf{r}, \mathbf{r}') q(\mathbf{r}') d^3 r'$ and $u^{\text{inc}}(\mathbf{r}) = \int G_0(\mathbf{r}, \mathbf{r}') q(\mathbf{r}') d^3 r'$. Here $u^{\text{inc}}(\mathbf{r})$ is the incident field, i.e., the field that would exist in the absence of inhomogeneities. Using $V = V_\alpha$, we obtain the following integral equation for $u(\mathbf{r})$:

$$u(\mathbf{r}) = u^{\text{inc}}(\mathbf{r}) - \int G_0(\mathbf{r}, \mathbf{r}') \delta\alpha(\mathbf{r}') u(\mathbf{r}') d^3 r' . \quad (34)$$

We then break up the sample into cubes C_n of side h , volume $v = h^3$, and denote the center of each cube by \mathbf{r}_n . The field $u(\mathbf{r})$ is approximated by a set of discrete values $u_n = u(\mathbf{r}_n)$. Setting $\mathbf{r} = \mathbf{r}_n$ in (34) and representing the volume integral as a sum of integrals over each voxel, we obtain

$$u_n = u_n^{\text{inc}} - \sum_m \int_{C_m} G_0(\mathbf{r}_n, \mathbf{r}) \delta\alpha(\mathbf{r}) u(\mathbf{r}) d^3 r , \quad (35)$$

where $u_n^{\text{inc}} = u^{\text{inc}}(\mathbf{r}_n)$. The above equation is, so far, exact. We now introduce several approximations. First, we replace $\delta\alpha(\mathbf{r}) u(\mathbf{r})$ in the integrand of Eq. (35) by $\delta\alpha_m u_m$, where $\delta\alpha_n = \delta\alpha(\mathbf{r}_n)$. Second, in all terms with $m \neq n$, we replace $G_0(\mathbf{r}_n, \mathbf{r})$ by $G_0(\mathbf{r}_n, \mathbf{r}_m)$. We then have

$$u_n = u_n^{\text{inc}} - \sum_{m \neq n} G_0(\mathbf{r}_n, \mathbf{r}_m) v \delta\alpha_m u_m - Q_n \delta\alpha_n u_n , \quad (36)$$

$$Q_n = \int_{C_n} G_0(\mathbf{r}_n, \mathbf{r}) d^3 r . \quad (37)$$

Note that the term with $m = n$ has been treated separately because the homogeneous medium Green's function $G_0(\mathbf{r}, \mathbf{r}')$ has a singularity at $\mathbf{r} = \mathbf{r}'$. The singularity is integrable and the quantity Q_n is well defined. However, the computation of Q_n is complicated due to the following two factors. First, $G_0(\mathbf{r}, \mathbf{r}')$ depends on the shape of boundaries and on the extrapolation distance ℓ in a complicated way and is not computable analytically in general. Second, the integration in (37) is over a cubic volume, while the asymptotic $\lim_{\mathbf{r} \rightarrow \mathbf{r}'} [G_0(\mathbf{r}, \mathbf{r}')] \propto 1/|\mathbf{r} - \mathbf{r}'|$ has spherical symmetry. The first difficulty is resolved by noting that G_0 is a sum of the Green's function in an infinite homogeneous space G_F and a contribution due to the boundaries G_B :

$$G_0(\mathbf{r}, \mathbf{r}') = G_F(\mathbf{r}, \mathbf{r}') + G_B(\mathbf{r}, \mathbf{r}') , \quad (38)$$

where G_F is given by (29). Accordingly, we can write Q_n as a sum of two contributions, Q_F and Q_{Bn} . Note that the Q_F is independent of the index n because the Green's function in an infinite homogeneous space is translationally invariant. The term Q_{Bn} can depend on n because boundaries break translational invariance, so that the integral in (37) can depend on \mathbf{r}_n . However, we will argue that Q_{Bn} is a small correction to Q_F . Indeed, $G_B(\mathbf{r}_n, \mathbf{r})$ can be written as a surface integral taken over the medium boundaries and has no singularity at $\mathbf{r} = \mathbf{r}_n$. We estimate that $Q_{Bn}/Q_F \sim (h/L_n) \exp(-k_d L_n)$, where L_n is the characteristic distance from the point \mathbf{r}_n to the medium boundary. We assume that all inhomogeneities are localized in a spatial region which is sufficiently far

from the medium boundaries. Then the ratio Q_{Bn}/Q_F is at least of the order of h/L_n ; if, in addition, $k_d L \gg 1$, this ratio is exponentially small. Therefore, we will neglect the term Q_{Bn} . The second difficulty is resolved by replacing the integration over the cube C_n by integration over a sphere of equivalent volume centered at \mathbf{r}_n . The radius of this sphere is $R_{eq} = (3/4\pi)^{1/3}h$. With these two approximations, and using (31), (32), we have

$$Q_n = Q_F = \frac{1}{k_d^2 D_0} f(k_d R_{eq}) , \quad (39)$$

where $f(x)$ is defined in (33). Note that for small x , $Q_F \approx R_{eq}^2/2D_0$.

Having computed Q_F , we can write a self-consistent “coupled-dipole equation” which is a discrete approximation to the integral equation (35).[‡] We define “dipole moments” $d_n = -vu_n\delta\alpha_n$, and, after some rearrangement of (36), obtain

$$d_n = \chi_n \left[u_n^{\text{inc}} + \sum_{m \neq n} G_0(\mathbf{r}_n, \mathbf{r}_m) d_m \right] , \quad (40)$$

$$\chi_n = -\frac{v\delta\alpha_n}{1 + Q_F\delta\alpha_n} . \quad (41)$$

In the above equation, χ_n plays the role of polarizability of the n -th dipole. In the absence of interaction, $d_n = \chi_n u_n^{\text{inc}}$. Note that the polarizability depends on $\delta\alpha_n$ nonlinearly due to the presence of the term $Q_F\delta\alpha_n$ in the denominator. A nonzero value of Q_F can be viewed as a result of interaction of the n -th dipole with itself and therefore can be referred to as the dipole self-energy. The physical effect of self-interaction is to limit the polarizability. Thus, the maximum (in absolute value) polarizability obtained in the limit $\delta\alpha_n \rightarrow \infty$ is $-v/Q_F$. We note that in the limit $k_d R_{eq} \rightarrow 0$, $Q_F\delta\alpha_n \ll 1$. In practice, the term $Q_F\delta\alpha_n$ can be small but not zero and should be accounted for.

We now return to operator notation. Let $|d\rangle$ be an N -dimensional vector of dipole moments d_n , $n = 1, \dots, N$, where N is the total number of voxels. Similarly, we define the N -dimensional vector $|u^{\text{inc}}\rangle$. We then have

$$|d\rangle = V_\alpha [|u^{\text{inc}}\rangle + G_0^{\text{VV}} |d\rangle] . \quad (42)$$

Here V_α and G_0^{VV} are $N \times N$ -matrices with elements

$$\langle n | V_\alpha | m \rangle = \chi_n \delta_{nm} , \quad (43)$$

$$\langle n | G_0^{\text{VV}} | m \rangle = (1 - \delta_{nm}) G_0(\mathbf{r}_n, \mathbf{r}_m) . \quad (44)$$

In the above formula, the superscript “VV” is an abbreviation for “volume-to-volume” and is used to emphasize that \mathbf{r}_n and \mathbf{r}_m are inside the discretized region. The formal solution to (42) is

$$|d\rangle = (I - V_\alpha G_0^{\text{VV}})^{-1} V_\alpha |u^{\text{inc}}\rangle . \quad (45)$$

[‡] In the case of the scalar field $u(\mathbf{r})$, a more appropriate term is “coupled-monopole equation” since the quantities d_n are, in fact, monopoles. We, however, adhere to the terminology used in electromagnetic scattering theory.

If there are N_s discrete sources located at the points \mathbf{r}_{sk} ($k = 1, \dots, N_s$) and N_d discrete detectors at points \mathbf{r}_{dl} ($l = 1, \dots, N_d$), we can write within the same precision as was used to discretize Eq. (35):

$$G^{\text{DS}} = G_0^{\text{DS}} + G_0^{\text{DV}} (I - V_\alpha G_0^{\text{VV}})^{-1} V_\alpha G_0^{\text{VS}}. \quad (46)$$

where the matrices G^{DS} , G_0^{DS} , G_0^{DV} and G_0^{VS} have the following elements:

$$\langle l | G^{\text{DS}} | k \rangle = G(\mathbf{r}_{dl}, \mathbf{r}_{sk}), \quad (47)$$

$$\langle l | G_0^{\text{DS}} | k \rangle = G_0(\mathbf{r}_{dl}, \mathbf{r}_{sk}), \quad (48)$$

$$\langle l | G_0^{\text{DV}} | n \rangle = G_0(\mathbf{r}_{dl}, \mathbf{r}_n), \quad (49)$$

$$\langle n | G_0^{\text{VS}} | k \rangle = G_0(\mathbf{r}_n, \mathbf{r}_{sk}). \quad (50)$$

Thus, G^{DS} and G_0^{DS} are matrices of size $N_d \times N_s$, G_0^{DV} is of size $N_d \times N$ and G_0^{VS} is of the size $N \times N_s$. The superscripts “VS” and “DV” stand for “source-to-volume” and “volume-to-detector”, respectively.

Eq. (46) is a discrete approximation to (16). We can identify

$$T = (I - V_\alpha G_0^{\text{VV}})^{-1} V_\alpha \quad (51)$$

as the discrete approximation to the T-matrix while V_α and G_0^{VV} as discrete N -dimensional approximations to the operators V_α and G_0 that were considered in Sections 2,3. We can further define the square root of V_α . For example, if $\delta\alpha_n$ are sign-definite, we write $V_\alpha = -\sigma S S$, where S is a diagonal matrix with the elements $|\chi_n|^{1/2}$. Then the T-matrix is written in the symmetric form (20) with $W = S G_0^{\text{VV}} S$. In the case of sign-indefinite $\delta\alpha_n$, we write the T-matrix in the form (22) with $W_c = S_c G_0^{\text{VV}} S_c$ and $V_\alpha = -S_c S_c$ (see Section 3.2).

The T-matrix can be computed by direct inversion of $I - V_\alpha G_0^{\text{VV}}$. This problem is well posed and has computational complexity $O(N^3)$. It should be stressed that computation of the T-matrix is completely independent of the sources and detectors and only requires knowledge of $\delta\alpha(\mathbf{r})$ and the unperturbed Green’s function $G_0(\mathbf{r}, \mathbf{r}')$. Once the T-matrix is found, the signal for any source-detector arrangement can be computed using (46) by direct matrix multiplication, an operation that can be performed with computational complexity $O[N^2 \min(N_d, N_s) + N N_d N_s]$. In a situation when the number of measurements is approximately equal to the number of unknowns, e.g., $N \sim N_s N_d$, the complexity of matrix multiplication is negligible compared to the complexity of computing the T-matrix.

The T-matrix approach to solving the forward problem has several advantages compared to finite differences or finite elements methods. First, only the spatial regions where inhomogeneities are supported need to be discretized. In this sense, the method is somewhat analogous to methods involving adaptive mesh generation. Second, once the T-matrix is computed, the measurable signal can be easily found for an arbitrary configuration of sources and detectors. However, unlike the finite difference and finite

elements methods, the T-matrix method requires knowledge of $G_0(\mathbf{r}, \mathbf{r}')$ which satisfies the proper boundary conditions. We note that G_0 can be found analytically for simple geometries or, in more complex cases, it can be computed numerically *once*, e.g., by finite differences or the finite-element method.

We conclude this section by noting that the discretized matrices W and W_c have zero trace, unlike their continuous counterparts whose traces are infinite. This is due to the renormalization procedure that was employed to remove the singularity of $G_0(\mathbf{r}, \mathbf{r}')$. Correspondingly, the sum of all eigenvalues of W or W_c is zero. Some of the eigenvalues of W are necessarily negative. In practice, we will see that W has many negative eigenvalues of very small absolute value and a much smaller number of positive eigenvalues. When $\delta\alpha_n \leq \alpha_0$, all eigenvalues are located in the unit circle.

7. Numerical Examples

We now illustrate the theoretical results of Section 3 with numerical examples using the discretization scheme of Section 6. All simulations have been performed in an infinite space, so that $G_0(\mathbf{r}, \mathbf{r}') = G_F(\mathbf{r}, \mathbf{r}')$, where G_F is given by (29). Physically, this corresponds to sources, detectors and the sample being immersed into an infinite homogeneous scattering medium. However, even if the sources and detectors are placed on the boundary (a diffuse-nondiffuse interface), the replacement of G_0 by G_F can be a reasonably accurate approximation if the boundaries are sufficiently far from the discretized region. Indeed, as was discussed in Section 6, G_0 can be written as a sum of G_F and G_B , where the boundary contribution G_B has no singularities when both of its argument are inside the medium but not on the medium boundary. Because $G_F(\mathbf{r}, \mathbf{r}')$ has a singularity at $\mathbf{r} = \mathbf{r}'$, it dominates G_B at small scales. Since the large-scale interaction is suppressed due to the exponential decay of diffuse waves, the input of boundaries is relatively insignificant for the computation of the T-matrix. However, computation of the *data function* (the measurable signal) according to the formula (46) can depend on boundary conditions very strongly. This is because elements of the matrices G_0^{DV} and G_0^{VS} are the Green's functions $G_0(\mathbf{r}_d, \mathbf{r})$ and $G_0(\mathbf{r}, \mathbf{r}_s)$ where \mathbf{r}_d and \mathbf{r}_s are located on the medium boundary.

For the specific choice $G_0 = G_F$, the T-matrix depends parametrically on $k_d^2 = \alpha_0/D_0$ but not on α_0 and D_0 separately. The same is true for W and W_c . The quantity k_d is known as the diffuse wave number and $\lambda_d = 2\pi/k_d$ as the diffuse wavelength; it gives the inverse scale on which diffuse waves exponentially decay. In all numerical examples shown below, λ_d sets the physical scale of the problem. The discretization step h is not a physical scale; it merely characterizes the precision to which we approximate the continuous field $u(\mathbf{r})$ by a set of discrete values u_n .

In the numerical simulations shown below, we have used LAPACK subroutines implemented in Intel's MKL library. In particular, we have used the routines DSYEVD and ZGEEV for diagonalization of real matrices W and complex symmetric matrices W_c , respectively. The computation time (on an 4×1.6 GHz Itanium-II HP rx4640 server)

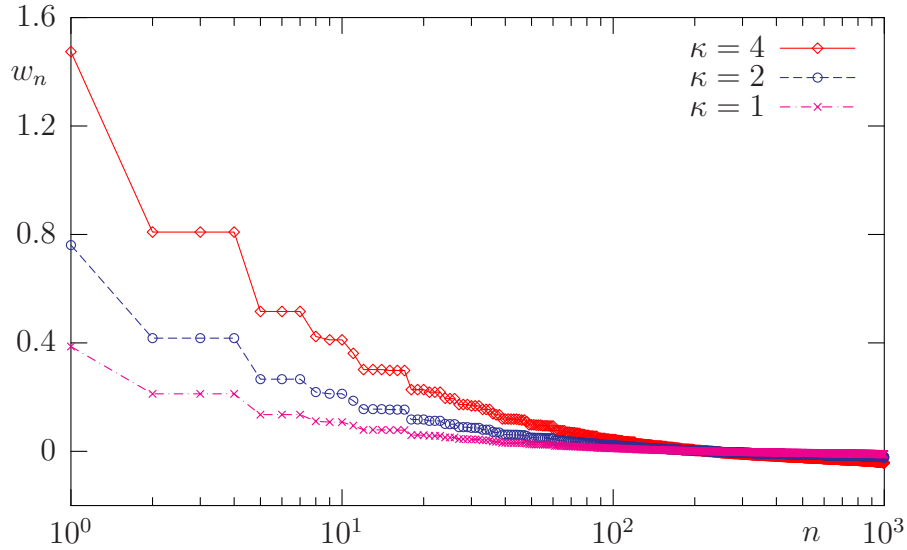


Figure 1. Eigenvalues w_n , in descending order, vs the eigenvalue number n , for an absorbing inhomogeneity of cubic shape of size $H = \lambda_d/2$ and various levels of contrast, κ . The target is discretized by 10^3 cubic voxels of size $h = \lambda_d/20$.

scaled approximately as $0.5(N/1000)^3 \text{sec}$ for SYEVD and $12(N/1000)^3 \text{sec}$ for ZGEEV. We have also employed the Rayleigh quotient to compute the maximum eigenvalue of the real matrix W . This method is quite reliable and can be used to find the maximum eigenvalue of matrices with $N \sim 70,000$ in approximately one minute (once the matrix G_0^{VV} is computed, which can take several additional minutes).

Although we show no directly relevant data, it is interesting to comment on the efficiency of computing the T-matrix by direct inversion of the matrix $A = I - V_\alpha G_0^{\text{VV}}$ according to (51). In the case of sign-definite $\delta\alpha$, factorization and subsequent inversion of A by the routines DPOTRF and DPOTRI is performed in approximately $0.14(N/1000)^3 \text{sec}$. For sign-indefinite $\delta\alpha$, the routines DGETRF and DGETRI were employed with a computational time of $0.19(N/1000)^3 \text{sec}$. Thus, computation of the T-matrix may be a highly efficient method of solving the forward problem of OT and can be applicable for discretization involving up to $\sim 10^4$ voxels. We stress that only the spatial regions that support inhomogeneities must be discretized. The computational disadvantage of the T-matrix approach is that the matrices G_0^{VV} and A are dense and require large storage and fast access to memory.

7.1. Sign-Definite Case

We start with the case when $\delta\alpha(\mathbf{r})$ does not change sign. Namely, we compute the real symmetric matrix W and find its eigenvalues for several shapes of $\delta\alpha(\mathbf{r})$.

The first example is an absorbing inhomogeneity (“target”) which has the shape of a single cube with side $H = \lambda_d/2$. It was assumed that $\delta\alpha(\mathbf{r}) = \kappa\alpha_0$ inside the cube and is zero outside. The target was approximated by 10^3 cubic voxels of volume h^3 . For this

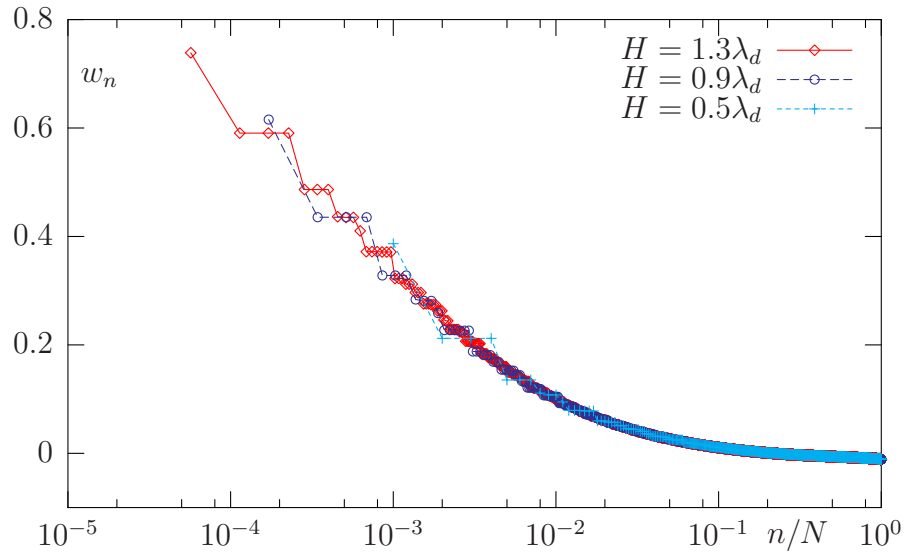


Figure 2. Eigenvalues w_n , in descending order, vs the *relative* eigenvalue number, n/N , where N is the size of the T-matrix, for an absorbing inhomogeneity of cubic shape, contrast $\kappa = 1$, and various side length H . The discretization step is $h = \lambda_d/20$.

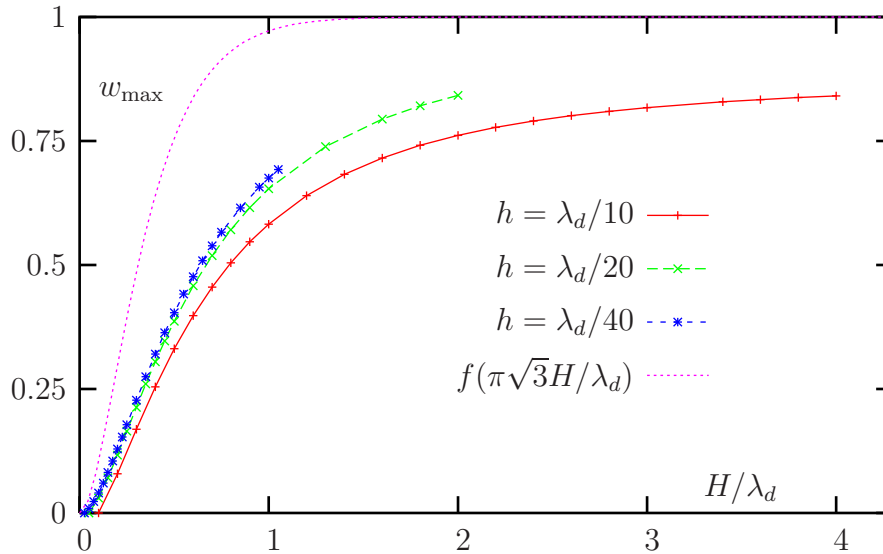


Figure 3. Maximum eigenvalue of W , w_{\max} , for a cubic target of contrast $\kappa = 1$ as a function the cube size H (relative to the diffuse wavelength λ_d) for different discretization.

discretization, $h = \lambda_d/20$, $k_d R_{\text{eq}} = 0.195$ and $Q_F \alpha_0 = 0.053$. The contrast κ was varied from 1 to 4. The eigenvalues of W are shown in Fig. 1. Note that for the minimum physically allowable contrast $\kappa = -1$, the eigenvalues differ from the case $\kappa = 1$ only very slightly due to the reversal of sign of the term $Q_F \delta \alpha_n$ in the denominator of (41) (data not shown). It can be seen that all eigenvalues satisfy $w_n < 1$ for $\kappa = 1$ with a large margin. Obviously, the eigenvalues are even smaller for $\kappa < 1$.

Next, we fix the contrast at $\kappa = 1$ and study the dependence of eigenvalues on the size of the cubic target, H . In Fig. 2, we plot eigenvalues for cubes of varying sizes H while the discretization step is fixed at $h = \lambda_d/20$. It can be seen that the maximum eigenvalue w_{\max} (the one with the lowest relative number) increases with the cube size but, for the set of parameters used, does not exceed unity. To study the behavior of w_{\max} in a broader range of parameters, we have used the Rayleigh quotient for various cube sizes and three different voxel sizes (see Fig. 3). The Rayleigh method is well suited for computing w_{\max} because of the large gap between the first two eigenvalues. The size of the cube was limited (depending on discretization) by the computational restriction on N . The maximum value of N used was $N = 74,088$. Approximately one fourth of all data points were verified by full diagonalization, with very good agreement. It follows from Fig. 3 that w_{\max} does not exceed unity for a very broad range of parameters. The curves $w_{\max}(H/\lambda_d)$ approach unity from below but appear to be unlikely to cross it. Note that inhomogeneities of sizes significantly larger than those used in Fig. 3 are rarely, if ever, encountered in OT experiments since the typical value of λ_d in biological tissues is 5cm. The visible difference between curves with $h = \lambda_d/10$ and $h = \lambda_d/20$ is due to the presence of the h -dependent self-energy $Q_F \delta \alpha_n$ in the denominator of (41). This term is comparable to unity for $h = \lambda_d/10$ but is already small for $h = \lambda_d/20$. Therefore, the difference between the $h = \lambda_d/40$ and the $h = \lambda_d/20$ curves is insignificant. Note that we expect that discretization with $h = \lambda_d/10$ is too rough to produce accurate results. However, the difference (or the lack of it) between the curves $w_{\max}(H/\lambda_d)$ with different h/λ_d can not be used *per se* to verify convergence of the T-matrix with h .

Since we have performed numerical simulations in infinite space, it is possible to compare $w_{\max}(H/\lambda_d)$ with the result that can be inferred from the convergence condition (2). To this end, we note the following. The data for Fig. 3 were computed for a cube of contrast $\kappa = 1$. If we increase the contrast by the factor γ , the Born series will still converge as long as $\gamma w_{\max} < 1$, or, equivalently, $\delta \alpha / \alpha_0 < 1/w_{\max}$. On the other hand, the convergence condition (2) has the form $\delta \alpha / \alpha_0 < 1/f(k_d a)$, where $f(x)$ is defined by (33) and a is the radius of the smallest sphere that circumscribes the cube of side H , namely, $a = \sqrt{3}H/2$. For these two conditions to be consistent, we must have $w_{\max}(H/\lambda_d) < f(\pi\sqrt{3}H/\lambda_d)$. The latter function is shown as a dotted line in Fig. 3.

Next, we consider the effects of multiple scattering of diffuse waves between two spatially separated absorbing inhomogeneities. To this end, we plot the spectrum of eigenvalues of W for two equivalent cubic targets of contrast $\kappa = 1$ and side $H = \lambda_d/2$, placed side-by-side and separated by the surface-to-surface distance ΔH . The targets were discretized using $h = \lambda_d/20$, so that each cube was approximated by 10^3 voxels. The results are shown in Fig. 4. When the cubes are sufficiently far apart ($\Delta H = H$), the interaction is weak and each eigenstate is doubly degenerate (this is in addition to the triple degeneracy of some eigenvalues which is due to the cubic symmetry). When the cubes approach, the degeneracy is broken by interaction. However, the effect of interaction is weak even when the two cubes approach each other very closely. At $\Delta H = 0$, the two cubes merge and form a single parallelepiped. At this point, the

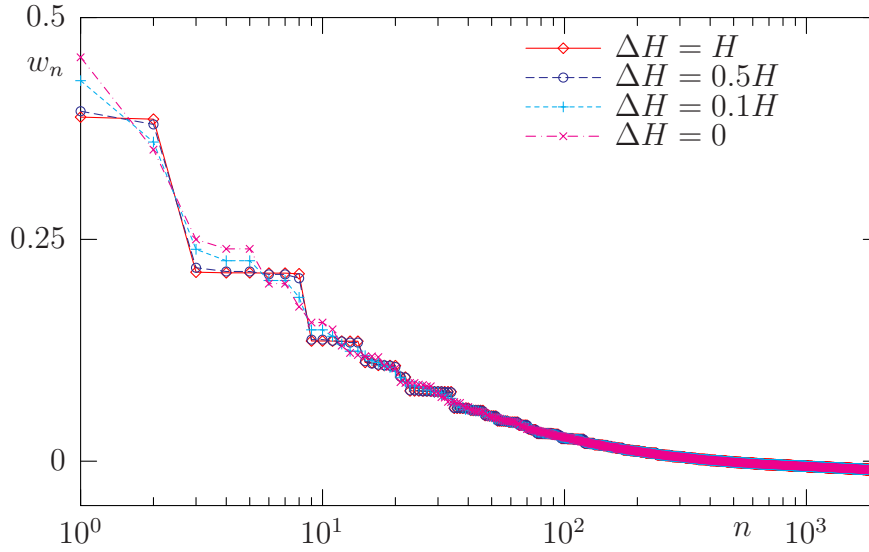


Figure 4. All eigenvalues w_n of the matrix W (in descending order) vs the eigenvalue number n for an absorbing inhomogeneity of contrast $\kappa = 1$ in the shape of two equivalent cubes of side $H = \lambda_d/2$ placed side-by-side and separated by the surface-to-surface distance ΔH . Each cube was discretized using $h = \lambda_d/20$ (10^3 voxels per cube).

maximum eigenvalue is increased only by 17% compared to the noninteracting limit. The weak interaction of spatially separated inhomogeneities is consistent with the idea of exponentially suppressed long-range interaction which was discussed in Section 3.1.

7.2. Sign-Indefinite Case

We now turn to the case of sign-indefinite $\delta\alpha(\mathbf{r})$. In this section, we will study the complex eigenvalues of the matrix W_c defined in Section 3.2. We note that, unlike in the case of W which is independent of the sign of $\delta\alpha$, $W_c[-\delta\alpha] = -W_c[\delta\alpha]$. Note that the eigenvalues of W_c change sign when the sign of $\delta\alpha$ is inverted.

The first example considered here is two cubic inhomogeneities similar to those used to compute the data points for Fig. 4, but now one of them has the negative contrast $\kappa = -1$. In Fig. 5, all eigenvalues of W_c for this system are shown as dots in the complex plane. When the cubes are sufficiently far apart, the imaginary parts of the eigenvalues are very small ($\sim 10^{-7}$ for $\Delta H = H$). This corresponds to the non-interacting limit, when the interaction operator W_c is, approximately, block-diagonal, where each block is real symmetric. As the cubes approach, some of the eigenvalues acquire imaginary parts. The eigenstates with complex eigenvalues are “hybridized”, i.e., they are collective eigenstates of the two interacting objects rather than “pure” eigenstates of each object taken separately. However, the hybridization is weak. Imaginary parts of the eigenvalues do not exceed 0.0015 in absolute value. Again, this is in agreement with the idea of exponentially-suppressed long-range interactions.

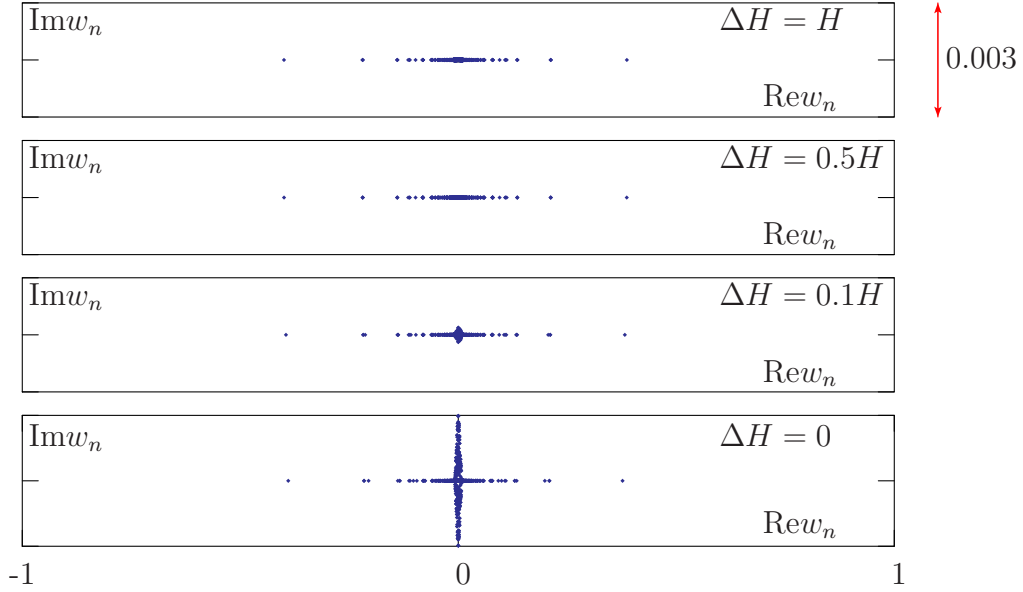


Figure 5. All eigenvalues of the matrix W_c for two cubic inhomogeneities of equal sides $H = 0.5\lambda_d$, placed side-by-side and separated by the surface-to-surface distance ΔH . One cube has contrast $\kappa = +1$ and the other $\kappa = -1$. Discretization: $h = \lambda_d/20$.

Next, we consider a layered structure of fifteen thin square layers of thickness h and alternating contrast $\kappa = \pm 1$ sandwiched on top of each other to form a cube of side $H = 0.75\lambda_d$. The discretization step is still $h = \lambda/20$. The eigenvalues of W_c are shown in Fig. 6. The displayed data indicate that there are hybridized eigenstates (those with complex eigenvalues) and eigenstates associated with an isolated thin layer and almost unaffected by the interaction (with almost purely real eigenstates). Overall, the absolute values of all eigenstates do not exceed 0.05. In this case, the matrix W is negligibly small compared to I and can be neglected. This corresponds to the first Born approximation, i.e., $T = V$. Thus, multiple scattering of diffuse waves for this layered structure is quite weak and can be neglected with little loss of precision.

The final example is one cubic inhomogeneity embedded inside another. Namely, a cube of size $11h \times 11h \times 11h$ with contrast $\kappa = -1$ was “coated” by a larger cube of size $21h \times 21h \times 21h$ with contrast $\kappa = +1$. The contrasts in the inner and outer cubes were not additive, so that $\kappa = -1$ in the interior and $\kappa = +1$ in the exterior of the structure. The discretization step was $h = \lambda_d/20$, so that the outer cube side was $H_{\text{out}} = 1.05\lambda_d$; the inner cube side was $H_{\text{in}} = 0.55\lambda_d$. The eigenvalues of the matrix W_c for this structure are shown in Fig. 7. Note that the vertical scale in this figure is the same as in Fig. 6, but the horizontal scale is ten times larger. Thus, while multiple scattering of diffuse waves inside each component (e.g., within the regions of positive or negative contrast) is much stronger than in the case of the layered structure of Fig. 6, hybridization is much weaker. The hybridized eigenvalues can be seen near the origin of the complex plane and are all very small in magnitude. At the same time,

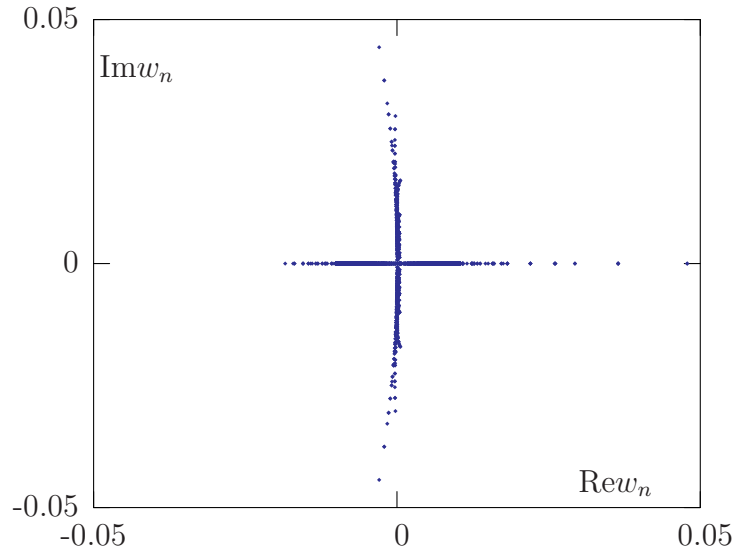


Figure 6. All eigenvalues of the matrix W_c for the layered absorptive inhomogeneity described in the text.

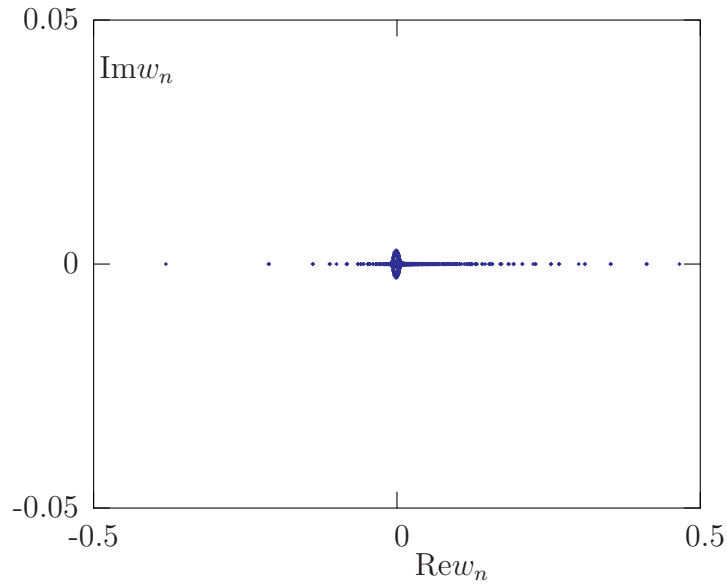


Figure 7. All eigenvalues of the matrix W_c for the absorptive inhomogeneity in the shape of two embedded cubes described in the text.

the eigenvalues that are relatively large in magnitude are almost purely real, which is characteristic for weak interaction between regions with positive and negative contrasts.

8. Discussion

In this paper, we have derived a sufficient condition for convergence of the Born series for the forward operator of optical tomography. The condition is quite simple and states that the series converge if the relative deviation of the absorption coefficient from

its background value $\delta\alpha(\mathbf{r})/\alpha_0$ does not exceed unity, independently of the support of $\delta\alpha(\mathbf{r})$. A similar condition was obtained for scattering inhomogeneities which are manifested by a spatially inhomogeneous diffusion coefficient. We have considered absorbing and scattering inhomogeneities separately; the situation when the absorption and the diffusion coefficients can vary in space simultaneously is not discussed in this paper. We argue that the convergence condition depends only on the amplitude but not on shape of $\delta\alpha$ (or δD) due to the exponential spatial decay of diffuse waves. Because of this decay, multiple scattering is suppressed on large scales. We emphasize again that we discuss here multiple scattering of diffuse waves – scalar solutions to the diffusion equation (3) – not electromagnetic multiple scattering which happens at much smaller physical scales. In the case when $\delta\alpha(\mathbf{r})$ has a compact support in a ball of radius a , a sharper convergence condition has been obtained (formula (2)), which is a generalization of the result previously obtained for the scalar wave equation [11]. A crucial difference between the convergence condition for propagating and diffuse waves is revealed in the limit $a \rightarrow \infty$, as is discussed in Section 5.

An interesting consequence of the convergence condition is that the nonlinearity of the inverse problem of optical tomography can be controlled if the constant α_0 can be controlled. Thus, increasing α_0 results in effective linearization of the inverse problem. Theoretically, α_0 can be chosen arbitrarily. However, the ill-posedness of the *linear* inverse problem tends to increase with α_0 . This reveals an interplay between the ill-posedness of the linearized inverse problem and the degree of nonlinearity of the full inverse problem (before linearization). Note that in experiments, α_0 can be tuned, for example, by changing the composition of an index-matching fluid.

We have performed numerical simulations for absorbing inhomogeneities. All numerical data are in agreement with the analytical results of this paper. We have found that the derived convergence condition is satisfied for a very broad range of parameters which are accessible in numerical experiments. We have also found that the effects of multiple scattering between spatially separated inhomogeneities such as two separate cubes is quite weak. This is again a consequence of the exponential decay of diffuse waves. Interaction of inhomogeneities whose contrasts have different signs was found to be especially weak. Thus, for the layered structure discussed in Section 7.2, the interaction is insignificant and the first Born approximation can be used with high accuracy – even though the object is a layered cube of size $H = 0.75\lambda_d$.

While we have found no substantial interaction between spatially separated inhomogeneities, nonlinearity can become strong in bulk inhomogeneities of large spatial extent or high contrast. In this case, the nonlinearity results from short-range interactions. Here two voxels can strongly interact with each other even if they are far apart, provided that there is a continuous path of other voxels connecting them.

Another aspect of the paper that deserves comment is the independence of the results on source-detector orientation. Indeed, it may seem natural that two absorbing cubes that block the line of sight will have more effect on the measured signal than the same two cubes rotated so that only one of them blocks the line of sight. In fact,

convergence or divergence of the Born series can be influenced, to a certain extent, by the source-detector arrangement. Indeed, calculation of the measurable signal according to (46) involves multiplication of the T-matrix by G_0^{DV} and G_0^{VS} from left and right. These matrices are source- and detector-dependent. It can happen that the matrix W has an eigenvalue larger than unity so that the Born series for the T-matrix diverges, but the corresponding eigenvector has a zero projection on either G_0^{DV} or G_0^{VS} . Then the Born expansion of the Green's function G^{DS} will converge for the selected source-detector configuration. However, if the Born series converges for the T-matrix, it converges for *all possible* source-detector pairs.

Finally, our results pertain only to convergence of the *forward series*. Analogous results on the convergence of the inverse series are not yet known.

Acknowledgment

This research was supported by the NSF grants DMS-0554100 and EEC-0615857.

References

- [1] Arridge S R 1999 *Inverse Problems* **15**(2) R41–R93
- [2] Gibson A P, Hebden J C and Arridge S R 2005 *Phys. Med. Biol.* **50** R1–R43
- [3] Roy R and Sevick-Muraca E M 2001 *Appl. Opt.* **40**(13) 2206–2215
- [4] Klose A D and Hielscher A H 2003 *Inverse Problems* **19**(2) 387–409
- [5] Ye J C, Webb K J, Bouman C A and Millane R P 1999 *J. Opt. Soc. Am. A* **16**(10) 2400–2412
- [6] Weglein A B, Gasparotto F A, Carvalho P M and Stolt R H 1997 *Geophysics* **62**(6) 1975–1989
- [7] Weglein A B, Araujo F V, Carvalho P M, Stolt R H, Matson K H, Coates R T, Corrigan R T, Corrigan D, Foster D J, Shaw S A and Zhang H 2003 *Inverse Problems* **19** R27–R83
- [8] Panasyuk G Y, Markel V A, Carney P S and Schotland J C 2006 *Appl. Phys. Lett.* **89**(22) 221116
- [9] Markel V A, O'Sullivan J A and Schotland J C 2003 *J. Opt. Soc. Am. A* **20**(5) 903–912
- [10] Bushell P J 1972 *J. Math. Phys.* **13**(10) 1540–1542
- [11] Colton D and Kress R 1998 *Inverse Acoustic and Electromagnetic Scattering Theory* vol 93 of *Applied Mathematical Sciences* (Berlin: Springer)
- [12] Markel V A and Schotland J C 2005 *Phys. Med. Biol.* **50** 2351–2364
- [13] Cuccia D J, Bevilacqua F, Durkin A J and Tromberg B J 2005 *Opt. Lett.* **30**(11) 1354–1356
- [14] Markel V A and Schotland J C 2004 *Phys. Rev. E* **70**(5) 056616(19)
- [15] Schotland J C 1997 *J. Opt. Soc. Am. A* **14**(1) 275–279
- [16] Gonatas C P, Ishii M, Leigh J S and Schotland J C 1995 *Phys. Rev. E* **52**(4) 4361–4365
- [17] Markel V A, Mital V and Schotland J C 2003 *J. Opt. Soc. Am. A* **20**(5) 890–902
- [18] Culver J P, Durduran T, Furuya T, Cheung C, Greenberg J H and Yodanis C L 2003 *J. of Cerebral Blood Flow and Metabolism* **23**(8) 911–924
- [19] Purcell E M and Pennypacker C R 1973 *Astrophys. J.* **186** 705–714
- [20] Draine B T 1988 *Astrophys. J.* **333** 848–872
- [21] Draine B T 2000 The discrete dipole approximation for light scattering by irregular targets, in *Light Scattering by Nonspherical Particles* (Academic Press)